Materials Transactions, Vol. 53, No. 3 (2012) pp. 513 to 517

Hydrogenation Properties of Ternary Intermetallic Compounds $Mg_{2-x}Pr_xNi_4$

N. Terashita[1], K. Sakaki[2], S. Tsunokake[1], Y. Nakamura[2] and E. Akiba[2,3]

[1]*Japan Metals & Chemicals Co., Ltd., Nishiokitama-gun, Yamagata 999-1351, Japan*
[2]*National Institute of Advanced Industrial Science and Technology, AIST Central 5, Tsukuba 305-8565, Japan*
[3]*Department of Mechanical Engineering, Faculty of Engineering, Kyushu University, Fukuoka 819-0395, Japan*

Ternary intermetallic compounds, $Mg_{2-x}Pr_xNi_4$ ($0.6 \leq x \leq 1.4$) were synthesized by induction melting and investigated with respect to hydrogenation properties and structural changes. These compounds have a cubic $C15_b$-type Laves structure (space group *F-43m*), where Mg and Pr have an ordered arrangement. The lattice parameters increased from $a = 0.70101(3)$ nm to $a = 0.71726(8)$ nm with increase of the Pr content. $Mg_{1.4}Pr_{0.6}Ni_4$ and $Mg_{1.2}Pr_{0.8}Ni_4$ absorbed and desorbed hydrogen up to ~0.7 H/M reversibly through one plateau in the *p-c* isotherms. The stoichiometric $MgPrNi_4$ showed two plateaus and its maximum hydrogen content reached to ~1.0 H/M at 35 MPa. The enthalpy changes of hydrides formation of $Mg_{1.4}Pr_{0.6}Ni_4$ and $Mg_{1.2}Pr_{0.8}Ni_4$ were estimated to be −39.2 and −40.3 kJ/mol H_2 respectively. The enthalpy changes of hydrides formation of $MgPrNi_4$ at the lower and higher plateaus were estimated to be −42.4 and −19.6 kJ/mol H_2 respectively. The metal sublattice of hydrides $Mg_{1.4}Pr_{0.6}Ni_4H_{\sim4}$ and $Mg_{1.2}Pr_{0.8}Ni_4H_{\sim4}$ had cubic ordered $C15_b$-type Laves structure same as the crystal structure before hydrogenation while hydride at the lower plateau of the stoichiometric $MgPrNi_4$ had an orthorhombic structure. The hydrogenation of $Mg_{0.8}Pr_{1.2}Ni_4$ and $Mg_{0.6}Pr_{1.4}Ni_4$ led to amorphization. [doi:10.2320/matertrans.M2011334]

(Received October 26, 2011; Accepted December 7, 2011; Published January 25, 2012)

Keywords: *hydrogen storage materials, Laves phases, induction melting, metal hydrides, pressure-composition isotherms, X-ray diffraction*

1. Introduction

Development of a hydrogen absorbing alloy which can reversibly absorb and desorb a large amount of hydrogen at ambient temperature and hydrogen pressure is an important subject to establish such hydrogen storage/transportation systems. It is of great interest to investigate novel Mg containing hydrogen absorbing alloys with a larger hydrogen storage capacity.

Recently various studies on the Mg containing hydrogen-absorbing alloys have been published. For example, hexagonal $PuNi_3$-type compounds $REMg_2Ni_9$ (RE = rare earth) were reported by Kadir *et al.*,[1–3] La–Mg–Ni system alloys were reported by Kohno *et al.*,[4] and the $C15_b$-type Laves phase $MgYNi_4$ was reported by Aono *et al.*[5] We also have developed the novel Mg containing alloys, $(Mg_{0.67}Ca_{0.33})Ni_2$ and $(Mg_{1-x}M_x)Ni_2$ (M = Ca, La, Ce, Pr, Nd and Gd) with C15 or $C15_b$-type Laves structure. Most of them reversibly absorb and desorb hydrogen at ambient temperature.[6,7] The maximum hydrogen content of $(Mg_{0.67}Ca_{0.33})Ni_2$ is 1.4 mass% (H/M = 0.7) under hydrogen pressure of 4 MPa at temperature of 278 K. We have improved plateau flatness and cycle durability of $(Mg_{0.67}Ca_{0.33})Ni_2$ C15-type Laves phase by substituting Y for a part of Ca.[8]

Hydrogenation properties of the ternary compounds $MgRENi_4$ (RE = La, Nd and Gd) have been reported by several groups.[9–12] However, the reported hydrogenation properties and structures are not necessarily consistent. It is probably because the quality of the samples depends on the synthesis methods. Because Mg has higher vapour pressure than the other constituent elements, to control the chemical composition of the products. Therefore the composition dependence of hydrogenation properties for $Mg_{2-x}RE_xNi_4$ has not been clear. More detailed investigation is necessary for understanding hydrogenation properties for $Mg_{2-x}RE_xNi_4$.

In this study, we have prepared $Mg_{2-x}Pr_xNi_4$ ($0.6 \leq x \leq 1.4$) homogeneous samples with accurate compositions using the advanced induction melting technique under helium atmosphere that can control the chemical composition of Mg based alloy more precisely. Their hydrogenation properties have been investigated to understand composition dependence on hydrogenation properties.

2. Experimental Procedure

2.1 Sample preparation

$Mg_{2-x}Pr_xNi_4$ compounds ($0.6 \leq x \leq 1.4$) were synthesized from elements of 99.9% or better purity by induction melting in a high-purity (purity > 96%) alumina crucible (1800 cc) and cast into a water-cooled iron board mold under 0.07 MPa helium (purity > 99.99%) atmosphere. This process has already been successfully industrialized. The shape of as-cast ingot was a flat plate 2–3 cm thick. The weight of each ingot was approximately 7–10 kg. In order to determine the suitable annealing conditions for as-cast alloys, melting points of each alloy were examined by differential thermal analyzer (DTA, Seiko Instruments Inc., EXSTAR6000). The annealing treatments were carried out at temperature 1223 and 1323 K for 10 h under an argon (purity > 99.999%) atmospheric flow. The resulting ingots were then powdered to proper sizes for pressure-composition isotherms (0.15–0.50 mm), X-ray diffraction profiles (>0.045 mm) and scanning electron microscopy (5–10 mm) by hand mill in the air.

2.2 Characterizations

The chemical compositions of the annealed alloys were analyzed by Inductively Coupled Plasma analyzer (ICP, Seiko Instruments Inc., SPS3100, SPS4000). The crystal structures, morphology and chemical compositions of each compound and each phase were characterized by powder X-ray diffraction (XRD, Rigaku Inc., RINT2000), scanning

Table 1 The results of chemical compositions analysis and annealing conditions of $Mg_{2-x}Pr_xNi_4$ ($x = 0.6$, 0.8, 1.0, 1.2 and 1.4).

Sample (target composition)	at%			Composition formula	Annealing condition
	Mg	Pr	Ni		
$Mg_{1.4}Pr_{0.6}Ni_4$	22.522	10.333	67.146	$Mg_{1.37}Pr_{0.63}Ni_{4.09}$	10 h at 1323 K under argon atomosphere
$Mg_{1.2}Pr_{0.8}Ni_4$	13.818	18.801	67.381	$Mg_{1.16}Pr_{0.84}Ni_{4.17}$	10 h at 1293 K under argon atomosphere
$MgPrNi_4$	16.823	16.637	66.540	$Mg_{1.01}Pr_{0.99}Ni_{3.98}$	10 h at 1323 K under argon atomosphere
$Mg_{0.8}Pr_{1.2}Ni_4$	19.917	13.997	66.086	$Mg_{0.83}Pr_{1.17}Ni_{3.91}$	10 h at 1173 K under argon atomosphere
$Mg_{0.6}Pr_{1.4}Ni_4$	9.986	23.373	66.641	$Mg_{0.56}Pr_{1.44}Ni_{4.12}$	10 h at 1223 K under argon atmosphere

electron microscopy (SEM, JEOL Ltd., JSM-6390A) and electron probe micro analyzer (EPMA, JEOL Ltd., JED2300), respectively.

The Pressure-Composition (p-c) isotherms were measured at temperatures 273–373 K in the pressure range from 2.0×10^{-3} to 35 MPa by automatic Sieverts'-type apparatus after few absorption/desorption cycles for activation. Hydrogen gas of purity higher than 99.9999% was used. The enthalpy and entropy change of each hydride formation were evaluated from van't-Hoff plot. Before and after measurements of p-c isotherms, XRD profiles were measured in the air to check whether samples showed hydrogen-induced amorphization, disproportionation and decomposition or not. In order to examine structural changes from alloy to hydride, we also measured XRD profiles of each hydride in the air. Each hydride was prepared by keeping under 8 MPa hydrogen in liquid nitrogen for a few hours after three times of absorption and desorption hydrogen cycles. The hydrogen content of each hydride after taking out in the air for the XRD measurements was determined by hydrogen analyzer (HORIBA, Ltd., EMGA-621W) consisting of electrical furnace and thermal conductivity detector.

3. Results and Discussions

3.1 Sample preparations

Table 1 shows the results of chemical analysis and annealing conditions. The results of chemical analysis agreed well with those of the target compositions. The difference from the target compositions with regard to the Ni content of samples was within 3 percent. Therefore in this study we are satisfied with the accuracy of chemical composition of the samples. This indicates that $Mg_{2-x}Pr_xNi_4$ compounds were synthesized without a heavy evaporation of Mg and reactions between alumina crucible and molten Mg during induction melting under helium atmosphere.

It should be pointed out that the estimation of the amount of evaporation of Mg during induction melting, exact control of molten metal temperatures, a period of melting time and sufficient stir are keys to successful synthesis by induction melting the alloys close to the target composition. It suggests that our applied estimations of a yield rate and melting conditions were suitable.

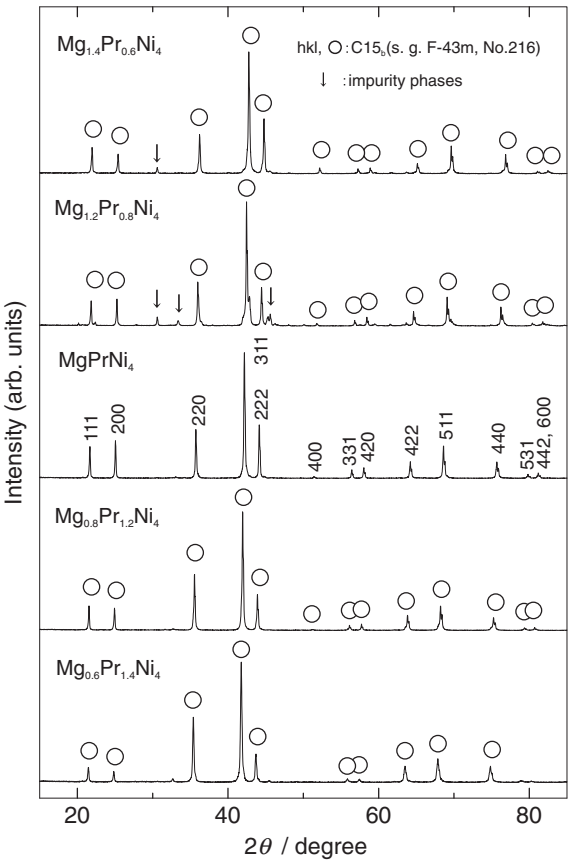

Fig. 1 XRD profiles of $Mg_{2-x}Pr_xNi_4$ ($x = 0.6$, 0.8, 1.0, 1.2 and 1.4) synthesized by induction melting and annealing. Open circles indicate the $C15_b$-type Laves phase.

3.2 Crystal structures

Figure 1 shows the XRD profiles of annealed $Mg_{2-x}Pr_xNi_4$. It can be seen that all compounds were close to a single phase with a $C15_b$-type Laves structure with space group *F-43m* (No. 216). However, there were small traces from impurity phases indicated by arrows.

The lattice parameters of the $C15_b$-type Laves phases of all compounds are listed in Table 2. The relation between the lattice parameters and the amount of the Pr content is shown in Fig. 2. The lattice parameters of the $C15_b$-type Laves phases increased with increasing the amount of Pr. Figure 2

Table 2 The hydrogen contents and the hydrides formation enthalpy and entropy evaluated from the van't-Hoff plots.

Sample	Lattice parameter at R.T. (nm)			Atomic radii ratio (R_A/R_B)
	before PCT measurement	hydride (metal atom substructure)	after PCT measurement	
$Mg_{1.4}Pr_{0.6}Ni_4$	$a = 0.70101(3)$	$a = 0.72852(8)$	$a = 0.70126(1)$	1.34
$Mg_{1.2}Pr_{0.8}Ni_4$	$a = 0.70590(4)$	$a = 0.7408(1)$	$a = 0.70596(3)$	1.36
$MgPrNi_4$	$a = 0.71024(2)$	orthorhombic (lower platrau) / cubic($C15_b$) (higher plateau)	$a = 0.71074(4)$	1.37
$Mg_{0.8}Pr_{1.2}Ni_4$	$a = 0.71375(1)$	amorphous		1.39
$Mg_{0.6}Pr_{1.4}Ni_4$	$a = 0.71726(8)$	amorphous		1.41

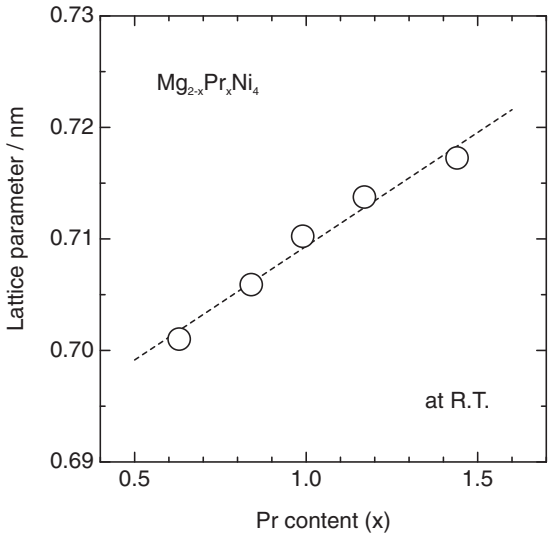

Fig. 2 The relation between the lattice parameter of $Mg_{2-x}Pr_xNi_4$ ($x = 0.6$, 0.8, 1.0, 1.2 and 1.4) and the amount of Pr.

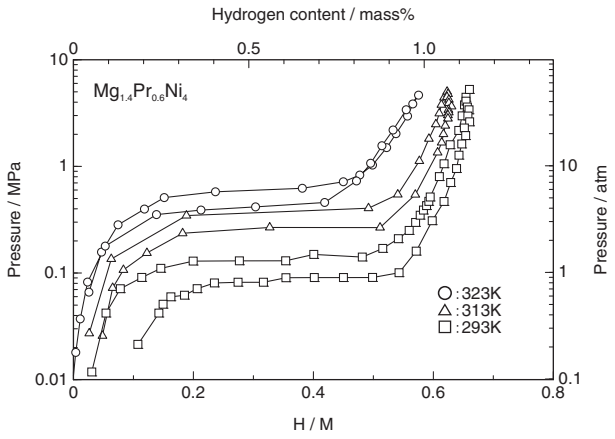

Fig. 3 *P-c* isotherms of $Mg_{1.4}Pr_{0.6}Ni_4$ at 293, 313 and 323 K.

clearly shows that the lattice parameters of $Mg_{2-x}Pr_xNi_4$ ($0.6 \leq x \leq 1.4$) obey the Vegard's law.

3.3 Hydrogenation properties

Figures 3, 4 and 5 show the *p-c* isotherms of $Mg_{2-x}Pr_xNi_4$ ($x = 0.6$, 0.8 and 1.0) up to 8 MPa at temperature range from 293 to 373 K. The hydrogen content of $Mg_{1.4}Pr_{0.6}Ni_4$,

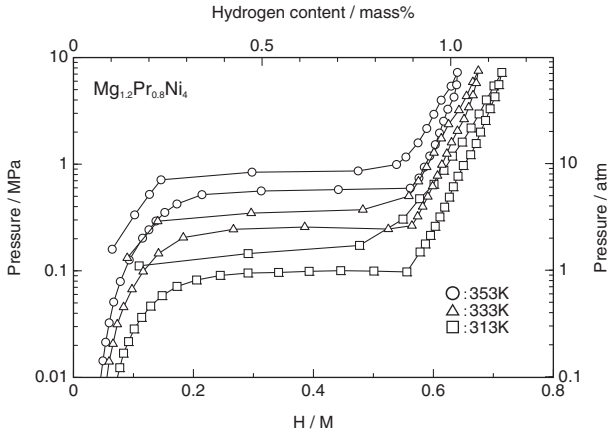

Fig. 4 *P-c* isotherms of $Mg_{1.2}Pr_{0.8}Ni_4$ at 313, 323 and 373 K.

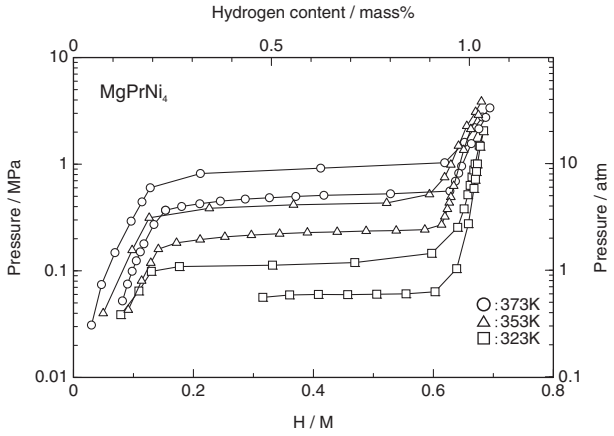

Fig. 5 *P-c* isotherms of $MgPrNi_4$ at 323, 353 and 373 K.

$Mg_{1.2}Pr_{0.8}Ni_4$ and $MgPrNi_4$ were 1.1 mass% ($H/M = 0.66$), 1.1 mass% ($H/M = 0.71$) and 1.0 mass% ($H/M = 0.68$), respectively. Furthermore, Fig. 6 shows the *p-c* isotherms of $MgPrNi_4$ up to 35 MPa at temperature of 273 and 298 K. These *p-c* isotherms showed distinct two plateaus, while $Mg_{1.4}Pr_{0.6}Ni_4$ and $Mg_{1.2}Pr_{0.8}Ni_4$ had only one plateau even if they were pressurized up to 35 MPa at the same temperature. The hydrogen content of $MgPrNi_4$ at 35 MPa and 273 K was 1.5 mass% ($H/M = 1.01$). On the other hand $Mg_{2-x}Pr_xNi_4$ ($x = 1.2$, 1.4) showed *p-c* isotherms without any plateau. The values of enthalpy changes of hydrides formation of $Mg_{1.4}Pr_{0.6}Ni_4$, $Mg_{1.2}Pr_{0.8}Ni_4$ and $MgPrNi_4$ at the lower

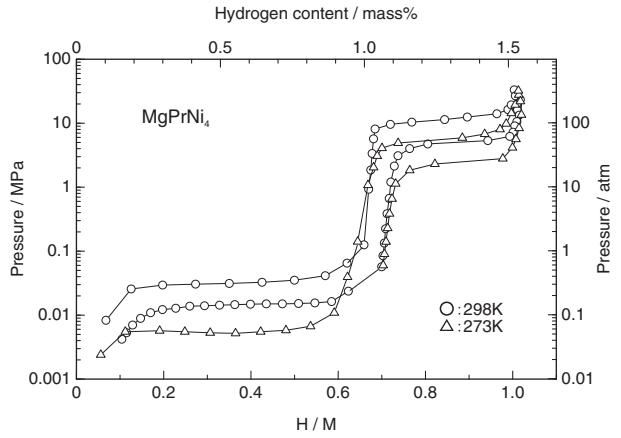

Fig. 6 *P-c* isotherms of stoichiometric $MgPrNi_4$ at 273 and 298 K up to 35 MPa.

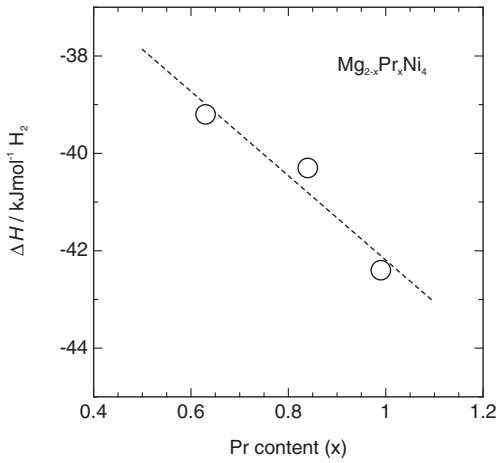

Fig. 7 The relation between the values of enthalpy changes of hydrides formation of $Mg_{2-x}Pr_xNi_4$ ($x = 0.6$, 0.8 and 1.0 at the lower plateau) and the amount of Pr content.

plateau were estimated to be −39.2, −40.3 and −42.4 kJ/mol H_2 respectively. The relation between the enthalpy changes of hydrides formation of $Mg_{2-x}Pr_xNi_4$ ($x = 0.6$, 0.8 and 1.0 at the lower plateau) and the amount of the Pr content is shown in Fig. 7. The values of enthalpy changes of hydrides formation decreased with increasing the amount of the Pr content. Moreover there is a linear correlation between the amount of the Pr content and the lattice parameters (cell volume). Accordingly the values of enthalpy changes of hydrides formation decreased with increasing the cell volume of $Mg_{2-x}Pr_xNi_4$. This relation was the same as conventional hydrogen absorbing alloys.[13] In addition the value of enthalpy changes of hydride formation of $MgPrNi_4$ at the higher plateau was estimated to be −19.6 kJ/mol H_2. The results of measurements of the *p-c* isotherms and the values of enthalpy and entropy change of each hydride formation are summarized in Table 3.

3.4 Structure change by hydrogenation

Figure 8 shows the XRD profiles of the hydrides of $Mg_{2-x}Pr_xNi_4$ ($x = 0.6$, 0.8, 1.0, 1.2 and 1.4). The lattice parameters of $C15_b$-type Laves phases before and after measurements of *p-c* isotherms, the lattice parameters of

Table 3 The lattice parameters of $C15_b$-type Laves phases before and after *p-c* isotherms measurements, lattice parameters of hydride phase and atomic radii ratios R_A/R_B of $Mg_{2-x}Pr_xNi_4$ ($x = 0.6$, 0.8, 1.0, 1.2 and 1.4).

Sample		Hydrogen content	Enthalpy and entropy change of hydride formation	
			ΔH (kJ/mol H_2)	ΔS^0 (J/mol H_2·K)
$Mg_{1.4}Pr_{0.6}Ni_4$		1.1 mass%, H/M = 0.66 (at 293 K, 5 MPa)	−39.2	−133.0
$Mg_{1.2}Pr_{0.8}Ni_4$		1.1 mass%, H/M = 0.71 (at 313 K, 7 MPa)	−40.3	−128.6
$MgPrNi_4$	lower plateau	1.0 mass%, H/M = 0.68 (at 323 K, 2 MPa)	−42.4	−126.8
	higher plateau	1.5 mass%, H/M = 1.01 (at 273 K, 35 MPa)	−19.6	−98.2

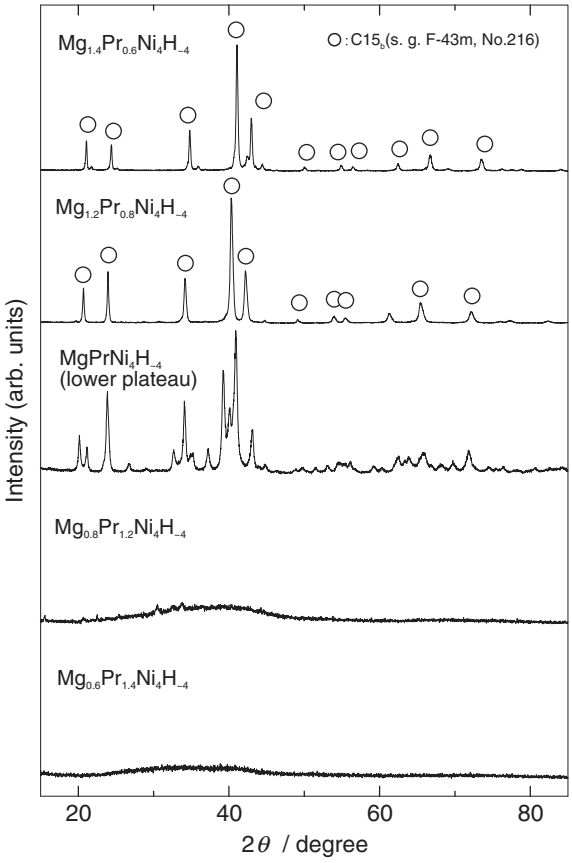

Fig. 8 XRD profiles of hydrides $Mg_{2-x}Pr_xNi_4H_{\sim 4}$ ($x = 0.6$, 0.8, 1.0, 1.2 and 1.4) measured in the air.

hydride phase and the value of R_A/R_B are summarized in Table 2. The metal sublattice of $Mg_{1.4}Pr_{0.6}Ni_4H_{\sim 4}$ and $Mg_{1.2}Pr_{0.8}Ni_4H_{\sim 4}$ showed the $C15_b$-type Laves structure same as the structure before hydrogenation. On the other hand, the metal sublattice of $MgPrNi_4H_{\sim 4}$ and $MgPrNiH_{\sim 6}$, the hydrides formed at the lower and higher plateau of the *p-c* isotherm, had an orthorhombic and cubic ($C15_b$-type) structure, respectively. The detailed structures of the two hydrides, $MgPrNi_4H_{\sim 4}$ and $MgPrNi_4H_{\sim 6}$, will be reported elsewhere.[14] XRD profiles of $Mg_{0.8}Pr_{1.2}Ni_4$ and $Mg_{0.6}Pr_{1.4}Ni_4$ after hydrogenation indicate that hydrogen-induced amorphization occurred in these compositions.

Aoki *et al.*[15,16] indicated that the ratio of the atomic radii, R_A/R_B, is a dominant factor for controlling the hydrogen-induced amorphization, where R_A and R_B are the atomic radii of A and B atoms in C15-type AB_2 Laves phases. When the value of R_A/R_B is larger than 1.37, hydrogen-induced amorphization occurs. In this study we assumed that R_A in $Mg_{2-x}Pr_xNi_4$ was average of atomic radii of Mg and Pr. The values of R_A/R_B for $Mg_{1.4}Pr_{0.6}Ni_4$ and $Mg_{1.2}Pr_{0.8}Ni_4$ were 1.34 and 1.36, respectively, both of which are smaller than 1.37. Actually hydrogen-induced amorphization did not occur in $Mg_{1.4}Pr_{0.6}Ni_4$ and $Mg_{1.2}Pr_{0.8}Ni_4$. The stoichiometric $MgPrNi_4$ has $R_A/R_B = 1.37$; hydrogen-induced amorphization did not occur, either. The values of R_A/R_B for $Mg_{0.8}Pr_{1.2}Ni_4$ and $Mg_{0.6}Pr_{1.4}Ni_4$ were 1.39 and 1.41, respectively, larger than 1.37. Hydrogen-induced amorphization was observed in both $Mg_{0.8}Pr_{1.2}Ni_4$ and $Mg_{0.6}Pr_{1.4}Ni_4$. The above empirical rule for hydrogen-induced amorphization is applicable to the $C15_b$ Laves phase $Mg_{2-x}Pr_xNi_4$.

4. Conclusions

From the experimental results the following conclusions can be drawn:

(1) $Mg_{2-x}Pr_xNi_4$ alloys were successfully synthesized by induction melting under helium atmosphere and annealing technique without discrepancy in target chemical composition. These compounds with $0.6 \leq x \leq 1.4$ have a cubic ordered $C15_b$-type Laves structures.

(2) When the Pr content increases, the lattice parameter of $Mg_{2-x}Pr_xNi_4$ $C15_b$-type Laves phases increases. It increases the equilibrium pressure and decreases the enthalpy changes of hydride formation. $Mg_{2-x}Pr_xNi_4$ with $x < 1$ reversibly absorbed and desorbed hydrogen through one plateau while the stoichiometric ($x = 1$) $MgPrNi_4$ showed two plateaus in the *p-c* isotherms. $Mg_{2-x}Pr_xNi_4$ with $x > 1$ showed *p-c* isotherms without any plateau.

(3) The metal sublattice of hydrides $Mg_{1.4}Pr_{0.6}Ni_4H_{\sim 4}$ and $Mg_{1.2}Pr_{0.8}Ni_4H_{\sim 4}$ has the $C15_b$-type Laves structure same as the alloy phase before hydrogenation while $MgPrNi_4$ transforms to $MgPrNi_4H_{\sim 4}$ with orthorhombic structure. In contrast, $Mg_{0.8}Pr_{1.2}Ni_4$ and $Mg_{0.6}Pr_{1.4}Ni_4$ become amorphous upon hydrogenation. The empirical rule of Aoki for hydrogen-induced amorphization based on the ratio of the atomic radii is applicable to the $C15_b$ Laves phase $Mg_{2-x}Pr_xNi_4$.

Acknowledgments

This work was supported by the New Energy and Technology Development Organization (NEDO) under "Development of technologies for hydrogen production, delivery and storage system" and "Advanced Fundamental Research Project on Hydrogen Storage Materials (HYDRO-STAR)".

REFERENCES

1) K. Kadir, T. Sakai and I. Uehara: J. Alloy. Compd. **257** (1997) 115–121.
2) K. Kadir, N. Kuriyama, T. Sakai, I. Uehara and L. Eriksson: J. Alloy. Compd. **284** (1999) 145–154.
3) K. Kadir, T. Sakai and I. Uehara: J. Alloy. Compd. **287** (1999) 264–270.
4) T. Kohno, H. Yoshida, F. Kawashima, T. Inaba, I. Sakai, M. Yamamoto and M. Kanda: J. Alloy. Compd. **311** (2000) L5–L7.
5) K. Aono, S. Orimo and H. Fujii: J. Alloy. Compd. **309** (2000) L1–L4.
6) N. Terashita, M. Takahashi, K. Kobayashi, T. Sasai and E. Akiba: J. Alloy. Compd. **293–295** (1999) 541–545.
7) N. Terashita and E. Akiba: Mater. Trans. **47** (2006) 1890–1893.
8) H. Tanaka, H. Senoh, N. Kuriyama, K. Aihara, N. Terashita and T. Nakahata: Mater. Sci. Eng. B **108** (2004) 81–90.
9) H. Oestrreicher and H. Bittner: J. Less-Common Met. **73** (1980) 339–344.
10) L. Guenee, V. Favre-Nicolin and K. Yvon: J. Alloy. Compd. **348** (2003) 129–137.
11) J.-L. Bobet, P. Lesportes, J.-G. Roquefere, B. Chevalier, K. Asano, K. Sakaki and E. Akiba: Int. J. Hydrogen Energy **32** (2007) 2422–2428.
12) J.-N. Chotard, D. Sheptyakov and K. Yvon: Z. Kristallogr **223** (2008) 690–696.
13) Y. Osumi, H. Suzuki, A. Kato, K. Ogura, S. Kawai and M. Kaneko: J. Less-Common Met. **89** (1983) 287–292.
14) K. Sakaki, N. Terashita, S. Tsunokake, Y. Nakamura and E. Akiba: J. Phys. Chem. C. in press.
15) K. Aoki, X.-G. Li and T. Masumoto: Acta Metall. Mater. **40** (1992) 1717–1726.
16) K. Aoki and T. Masumoto: J. Alloy. Compd. **194** (1993) 251–261.